ANP32 proteins are essential for influenza virus replication in human cells

Ecco Staller[a], Carol M Sheppard[a] , Peter J Neasham[a], , Bhakti Mistry[a], Thomas P Peacock[a], Daniel H Goldhill[a], Jason S Long[a], and Wendy S Barclay[a]#

[a]Section of Molecular Virology, Imperial College London, St Mary's Campus, London, UK

Running Head: ANP32 proteins essential for influenza replication

#Address correspondence to Wendy S Barclay, w.barclay@imperial.ac.uk

Abstract: 179 words

Text: 4216 words

Abstract ANP32 proteins have been implicated in supporting influenza virus replication, but most of the work to date has focused on the ability of avian Anp32 proteins to overcome restriction of avian influenza polymerases in human cells. Using a CRISPR approach we show that human ANP32A and ANP32B are functionally redundant but essential host factors for mammalian-adapted influenza A virus (IAV) and influenza B virus (IBV) replication in human cells. When both proteins are absent from human cells, influenza polymerases are unable to replicate the viral genome, and infectious virus cannot propagate. Provision of exogenous ANP32A or –B recovers polymerase activity and virus growth. We demonstrate that this redundancy is absent in the murine Anp32 orthologues: murine Anp32A is incapable of recovering IAV polymerase activity, while murine Anp32B can. Intriguingly, IBV polymerase is able to use murine Anp32A. We show using a domain swap and point mutations that the LRR 5 region comprises an important functional domain for mammalian ANP32 proteins. Our approach

has identified a pair of essential host factors for influenza virus replication and can be harnessed to inform future interventions.

Importance Influenza virus is the etiological agent behind some of the most devastating infectious disease pandemics to date, and influenza outbreaks still pose a major threat to public health. Influenza virus polymerase, the molecule that copies the virus RNA genome, hijacks cellular proteins to support its replication. Current anti-influenza drugs are aimed against viral proteins, including the polymerase, but RNA viruses like influenza tend to become resistant to such drugs very rapidly. An alternative strategy is to design therapeutics that target the host proteins that are necessary for virus propagation. Here we show that the human proteins ANP32A and ANP32B are essential for influenza A and B virus replication, such that in their absence cells become impervious to the virus. We map the pro-viral activity of ANP32 proteins to one region in particular, which could inform future intervention.

Journal of Virology JVI Journal of Virology

Introduction

Influenza viruses are a major cause of respiratory illness and mortality worldwide, causing approximately 500,000 deaths annually from seasonal epidemics alone (1). An additional and potentially much more serious burden arises from zoonotic emergence of pandemic viruses from birds, the natural reservoir of influenza viruses. The most notorious of these events, in 1918, claimed the lives of an estimated 50 million people, while the latest pandemic to date, in 2009, killed over 250,000 worldwide (2). In order to mitigate the impact of the next influenza pandemic and reduce the seasonal burden, new approaches to thwart influenza virus are required. A first step toward novel treatment is an enhanced understanding of the interactions between virus and host cell.

Influenza virus requires the host cell machinery to support replication of its genome and production of new virions. The influenza genome is made up of eight segments of single-stranded negative sense RNA (vRNA). Each segment is packaged in a double helical loop structure bound by nucleoprotein (NP) along its length, except for the pseudo-complementary 3' and 5' untranslated regions that comprise the promoter (3-5). These termini instead associate with an RNA-dependent RNA polymerase (RdRp) encoded by the virus (6). This key enzyme, a heterotrimer of polymerase basic 1 (PB1), polymerase basic 2 (PB2), and polymerase acidic (PA) functions as both a transcriptase and a replicase (reviewed in (7)). Transcription of mRNA and replication through a positive-sense complementary RNA (cRNA) take place in the host cell nucleus (7, 8). A viral complex containing RNA, NP, and RdRp is termed a ribonucleoprotein (RNP), which, depending on the sense of the RNA, is either a vRNP or a cRNP.

ANP32A and ANP32B are small acidic nuclear phosphoproteins that are attributed to a plethora of cellular functions (9), including chromatin remodelling (10, 11), apoptosis (12, 13),

transcription regulation (14, 15), and intracellular transport (16). ANP32 proteins are approximately 250 amino acids in length, and contain an N-terminal leucine-rich repeat (LRR) region, a central domain, and an unstructured low-complexity acidic region (LCAR) at the C terminus. ANP32 proteins have been associated with influenza A polymerase function. A nuclear fraction containing ANP32A and B was shown to enhance the synthesis of vRNA from a short complementary RNA (cRNA) template *in vitro* (17). Knockdown of ANP32A or B in human cells reduced polymerase activity measured in minigenome reporter assays, as well as synthesis of viral RNA in infected cells (17, 18). Direct interactions of ANP32 proteins with the RdRp or RNP have been documented but do not completely correlate with function (19-22). The difference between avian and mammalian ANP32A proteins has been suggested to account for host range restriction of avian influenza strains in mammalian cells, and much of the work to date has focused on the avian orthologues, particularly chicken (23).

Here we use CRISPR/Cas9 genome editing to render the *Anp32A* and/or *Anp32B* genes non-functional in low-ploidy human eHAP1 cells (24, 25), thus obtaining a clean experimental platform in which to investigate the interplay between different influenza virus polymerases and mammalian ANP32 proteins. We find that although IAV and IBV polymerases can replicate in the absence of either ANP32A or ANP32B alone (i.e. in single knockout cells), depletion of both proteins (double knockout) renders the cell impervious to RdRp activity. Furthermore, none of the IAV strains tested is capable of replication in the double knockout cells. Human ANP32A and –B proteins are thus functionally redundant but essential for influenza virus replication. We further show that this redundancy is not present in the murine Anp32 orthologues. Only murine Anp32B (MusB) is able to recover IAV polymerase activity, although surprisingly murine Anp32A (MusA) can be co-opted by IBV polymerase. Functionality mapped to leucine-rich

repeat 5 of the LRR domain, thus assigning this domain of the host proteins as key for the support of influenza polymerase activity and a target for future interventions.

Results

Generation of eHAP1 knockout cells eHAP1 cells lacking ANP32A (AKO), ANP32B (BKO), or both proteins (dKO) were generated by CRISPR/Cas9 genome editing using a double nickase approach for enhanced specificity and minimal off-target DNA cleavage (26, 27) (Figure 1a). Control cells (control) were treated in identical manner with non-targeting guide RNAs (28). Two independent clones with diallelic disruption of the *Anp32A* or *Anp32B* locus were verified by NGS and Sanger sequencing of individual alleles, and loss of protein expression confirmed by Western blotting against ANP32A or ANP32B, respectively (Figure 1b and data not shown). Double knockout cells were generated by tandem CRISPR from a BKO clone, using the guides against the *Anp32A* locus. Three independent dKO clones were verified by Sanger sequencing and loss of expression was confirmed by Western blot analysis (Figure 1b and data not shown).

Influenza virus polymerase activity is dependent on either ANP32A or ANP32B Minigenome reporter assays were carried out in single and double ANP32 knockout cells with reconstituted polymerases from three different influenza A viruses – a seasonal H3N2 virus (A/Victoria/3/75), an avian H5N1 virus (A/turkey/England/50-92/1991) with the mammalian-adapting mutation E627K in the PB2 subunit, and a 2009 pandemic H1N1 virus (A/England/195/2009) – as well as an influenza B virus (B/Florida/04/2006). Surprisingly, absence of ANP32A in human cells did not result in loss of influenza polymerase activity; in fact activity increased for some polymerase constellations. (Figure 1c-f). Polymerase activity in BKO clones was either unaffected or decreased but not abrogated (Figure 1c-f). A similar pattern was observed in A549 cells lacking ANP32A or ANP32B (data not shown). Strikingly, however, none of the polymerases showed any activity in three independent double knockout lines (Figures 1c-f and data not shown), despite robust expression of vRNP components (Figure 1c-f).

106 These data suggest functionally redundant roles for ANP32A and ANP32B in supporting
107 influenza virus polymerase activity in human cells.

108 In order to confirm redundancy, polymerases were co-expressed in dKO cells with plasmids
109 encoding exogenous ANP32A, ANP32B, or equal amounts of both. All polymerases tested
110 regained activity in the presence of either ANP32 protein (Figure 2a-d). Provision of both
111 proteins at once did not further enhance rescue. These results were corroborated at single cell
112 level: ANP32A or -B proteins fused to the red fluorescent protein mCherry were co-expressed in
113 dKO cells with H5N1 (PB2 627K) 50-92 vRNP components PB1, PB2-627K, PA-GFP, and NP,
114 with an influenza minigenome encoding blue fluorescent protein (BFP) as a reporter. Blue
115 fluorescence resulting from active polymerase was observed only in cells that expressed ANP32
116 proteins, and either paralogue was able to rescue activity (Figure 2e).

117 These data demonstrate that ANP32A and -B proteins are essential but redundant for influenza A
118 and B polymerase activity in human cells. Intriguingly, we observed recovery of polymerase
119 activity in dKO cells was more efficiently achieved by expression of ANP32B than ANP32A for
120 specific polymerase constellations, namely avian H5N1 50-92 (PB2 627K) and IBV Florida 06
121 (Figure 2b and d). These two polymerase constellations were also more affected by loss of
122 ANP32B expression (Fig 1d and f), suggesting ANP32B is the preferred host factor for these
123 polymerases in human cells.

124 **IAV replication is abrogated in cells lacking ANP32A and ANP32B** To investigate the
125 consequence of absence of ANP32A or -B proteins on infectious IAV replication in human cells,
126 control, single, and double knockout cells were infected at MOI = 0.005 with three different
127 viruses whose genetic content corresponded to the polymerase constellations tested in Figures 1
128 and 2, i.e. from Vic/75, Tky/50-92 (E627K) or Eng195. While virus replicated to high titres in

129 control and single KO cells, replication in dKO cells was completely abrogated (Figure 3a-c)).
130 This suggests that viral proteins such as NEP and NS1 (expressed during virus infection but not
131 provided in the minigenome assay) cannot overcome the block in replication imposed by the
132 absence of ANP32 proteins. Replication of the H1N1 laboratory-adapted strain A/PR/8/34 was
133 also abrogated in dKO cells (data not shown). Reconstitution of dKO cells with both ANP32 A
134 and B proteins by transient transfection prior to infection restored PR8 virus replication (Figure
135 3d).

136 It has been suggested that ANP32A and –B specifically support the synthesis of negative-sense
137 vRNA from a positive-sense intermediate template (cRNA) (17). This is believed to occur after
138 primary transcription *in cis* of the vRNA by the incumbent RdRp, and requires newly
139 synthesised RdRp molecules to stabilise the cRNA *in trans* (29, 30). Therefore, without
140 replication, secondary transcription and accumulation of viral proteins will not occur. We used
141 immunofluorescence microscopy to visualise accumulation of viral nucleoprotein (NP) in control
142 and dKO cells, five hours post-infection with H1N1 PR8 virus. NP accumulation exceeded
143 background level only in cells containing ANP32 proteins (Figure 4a), but this approach was not
144 sufficiently sensitive to image NP protein products of primary transcription. In order to assess
145 which viral RNAs were synthesized in cells that lack expression of ANP32 proteins, we pre-
146 expressed an inactive influenza polymerase complex (to stabilize any cRNA generated) for 20
147 hours before infecting with high MOI virus in presence or absence of cycloheximide (CHX). 5
148 hours later, levels of v, c, and mRNAs generated from segment 6 of the incoming virus were
149 assayed by qRT-PCR (Figure 4b). In control cells, amplification of all 3 RNA species was
150 evident in absence of CHX. In dKO cells, RNA levels were not different in presence or absence
151 of CHX, indicating that vRNA was not replicated. Primary transcription of mRNA and

pioneering round generation of cRNA were detected in dKO cells since RNA levels were similar to those detected in presence of CHX in control cells. Thus our data support the block to replication occurring at the step of copying cRNA back to vRNA in absence of ANP32 proteins.

Murine Anp32B supports IAV polymerase We used the complementation assay in dKO cells to ask whether Anp32 proteins from non-human species relevant to influenza virology were capable of supporting polymerase function. We carried out minigenome reporter assays co-expressing Anp32A proteins from pig (SusA), mouse (MusA), duck (AnasA), and chicken (GallusA) with IAV polymerase (H3N2 Victoria/75). While the avian and porcine orthologues could support IAV polymerase, MusA could not (Figure 5a). Bearing in mind that our results suggest that human ANP32B might be the more potent host factor for some polymerase constellations, we hypothesised that in mice, influenza virus might rely solely on MusB to support its replication. Indeed, expression of MusB could recover Vic/75, polymerase activity in dKO cells (Figure 5b), despite equal levels of expression of both murine Anp32 proteins and their localisation to the cell nucleus (Figure 5b and c).

An alignment of murine and human ANP32 proteins showed several unique features in the MusA sequence, mapping largely to surface-exposed residues within LRR 5 (Figure 5d. In order to determine whether these differences were responsible for the lack of functionality of MusA, we generated a chimera of murine Anp32A and B ($MusA^{128-153}$) by substituting a 26-amino acid segment (aa 128-153) of MusB into MusA (Figure 5d), and then tested if this conferred gain of function on MusA to support IAV polymerase. The chimera was indeed capable of recovering activity of Vic/75 polymerase in dKO cells, although not to the level shown by MusB (Figure 5b).

174 Western blot and immunofluorescence analysis of the FLAG-tagged chimeric construct
175 demonstrated expression and nuclear localisation (Figure 5 b and c).

176 We identified a single amino acid in LRR5 at position 130 that was the same in human ANP32A
177 or B and MusB (aspartic acid, D) but differed in MusA (alanine, A) (Figure 5e and f).
178 Introduction of a D130A single point mutation in huANP32Asignificantly reduced its ability to
179 support Vic75 polymerase activity, and conversely introduction of A130D to MusA produced a
180 small but significant increase in its ability to support viral polymerase (Figure 5g).

181

182 Finally, we explored whether MusA or MusB could support activity of polymerases derived from
183 other IAV strains or from IBV. As seen for Vic/75 polymerase, MusA was non-functional for
184 IAV polymerases from A/Tky/50-92/91 and A/Eng/195 (Figures 6a and b), however IBV Florida
185 06 polymerase recovered some activity in dKO cells in the presence of MusA (Figure 6c). MusB,
186 however, was the more potent factor for support of IBV polymerase. Intriguingly, IBV Florida
187 06 polymerase activity was even greater in the presence of the MusA/B chimera than MusB
188 (Figure 6c)

189

Discussion

Here we show that human ANP32A and ANP32B are functionally redundant in their support for influenza virus polymerase in human cells, and that the RdRp does not carry out RNA replication in the absence of both family members. Our findings corroborate those of Zhang et al. (2019) who have used a similar CRISPR approach(31) We further show that IBV polymerase is also dependent on human ANP32 proteins and can also utilize either orthologue to support activity. Our demonstration of redundancy in use of these essential host factors illuminates a deficiency in RNAi or CRISPR screens where host genes are knocked down one at a time. Functionally redundant pairs or larger groups of host factors that can be used by a virus will escape detection, as have ANP32A and B individually in previous screens (33, 34)

Two observations imply preference of certain polymerase constellations for human ANP32B over ANP32A. First, specific polymerases were more efficiently enhanced by ANP32B when provided exogenously. Second, the absence of ANP32A in the cell enhances virus polymerase activity in some cases, where the opposite might be expected and has previously been observed in knockdown experiments (17, 18). The latter observation might be explained if ANP32B is held in heterodimers or larger protein complexes with ANP32A, thus absence of ANP32A might liberate the preferred ANP32B for recruitment by influenza virus RdRp. Alternatively, ANP32A and B, being very similar structurally, might compete for polymerase binding, and loss of ANP32A would then favour binding and more efficient activity mediated by ANP32B. Taken together the observations point to ANP32B being functionally superior for supporting influenza polymerase than ANP32A in humans. However, these differences were not so readily apparent in the context of virus infection where replication continued largely unabated in single ANP32A or B knockout cells.

213 Interestingly, the redundancy observed in humans is not observed for murine Anp32 proteins.
214 IAV polymerases cannot use MusA, but IBV polymerase can, albeit inefficiently. The ability of
215 influenza A virus to replicate in mice is explained by the utility of murine Anp32B. Mapping this
216 difference using a chimeric approach revealed LRR 5 as a key domain of ANP32 proteins for
217 supporting IAV polymerase, and point mutation highlighted the role of a single amino acid in
218 LRR 5 at position 130. It will be important to investigate whether this is a contact point in the
219 interaction between the viral complex and the host protein, and this will be a crucial question for
220 structural studies to address. The highlighted domain sits adjacent to a linker region between the
221 structured LRR and highly flexible LCAR, and may be important for defining overall structural
222 arrangement and susceptibility to conformational change. It is interesting to note that in chicken
223 cells, it is the Anp32A orthologue that is utilized by avian influenza polymerase, whereas
224 chAnp32B does not support replication, and this difference in functionality was also mapped to
225 LRR 5 (31, 32,).

226 Current anti-influenza therapeutics, and drugs in development, such as adamantanes (M2 ion
227 channel inhibitors), neuraminidase inhibitors (NAIs) such as oseltamivir, and RdRp-targeting
228 molecules (including the nucleoside analogue favipiravir and small molecules such as Baloxavir)
229 are all aimed at proteins encoded by the virus. A recurring issue with such drugs is the ease with
230 which influenza virus evolves resistance to them, be it in a laboratory setting (36) or in the field
231 (37-39). An alternative approach would be to target specific interactions of virus proteins with
232 essential host factors, such that small molecule inhibitors may temporarily block the interacting
233 surface on the host protein, without compromising its cellular functions. As influenza virus
234 replication is completely abrogated in their absence, ANP32 proteins suggest themselves as
235 potential candidates for such an approach.

236

Materials and Methods

Cells and cell culture

Human eHAP1 cells (Horizon Discovery) were cultured in Iscove's Modified Dulbecco's Medium (IMDM; ThermoFisher) supplemented with 10% fetal bovine serum (FBS; labtech.com), 1% non-essential amino acids (NEAA; Gibco), and 1% penicillin/streptomycin (Invitrogen). Human lung adenocarcinoma epithelial cells (A549) (ATCC) and Madin-Darby canine kidney (MDCK) cells (ATCC) were maintained in Dulbecco's modified Eagle's medium (DMEM; Invitrogen) supplemented with 10% FBS, 1% NEAAs, and 1% penicillin-streptomycin (Invitrogen). All cells were maintained at 37 °C in a 5% CO_2 atmosphere.

Plasmids and cloning

cDNAs of full-length human codon-optimised murine Anp32A and B isoforms were generated by gene synthesis (GeneArt, ThermoFisher) using sequences NP_033802.2 (mouse Anp32A) and NP_570959.1 (mouse Anp32B) and cloned into pCAGGS expression plasmids including a C-terminal GSG linker followed by a FLAG tag and 2 STOP codons. Human pCAGGS ANP32A and B, chicken Anp32A, pig Anp32A, and duck Anp32A expression plasmids have been described (18). The chimeric mouse construct and human ANP32A and B point mutants were cloned by overlapping PCR, using primers CCAACCTGAATGCCTACCGCGAGAAC and GTTCTCGCGGTAGGCATTCAGGTTGG (huANP32A-D130A), CAAACCTGAATGCCTATCGGGAGAGC and GCTCTCCCGATAGGCATTCAGGTTTG (huANP32B-D130A), GGTCACTTCGCAGTTAAACAAATCCAG, GTTTAACTGCGAAGTGACCAACAGAAGC, GCCCTCCACGTCGCTGTCAGGGGCCTC, and GACAGCGACGTGGAGGGCTACGTGGAG (mouse Anp32A/Anp32B domain swap).

Mouse ANP32A mutant A130D was generated by overlapping PCR using primers GGTAACCAACCTTAATGATTACCGGGAGAACGTC and GACGTTCTCCCGGTAATCATTAAGGTTGGTTACC. pCAGGS expression plasmids encoding each polymerase component and NP for H3N2 Victoria, H5N1 (PB2-627K) 50–92, pH1N1 England 195, and IBV Florida 06 have been described (40, 41) pPolI reporter plasmids containing firefly luciferase or blue fluorescent protein flanked by IAV or IBV-specific promoters have been described (42). All plasmid constructs were verified by Sanger sequencing and analysed manually in Geneious v6.

Generation and screening of CRISPR clones

Pairs of guide RNAs against exon 2 of human *Anp32A* (GTCAGGTGAAAGAACTTGTCC and GAAGGCCCGACCGTGTGAGCG) and *Anp32B* (GAGCCTACATTTATTAAACTG and GCAAGCTGCCTAAATTGAAAA) were designed with the aid of the CRISPR design tool at www.crispr.mit.edu (Feng Zhang Lab). The non-targeting guide RNA pair was GTATTACTGATATTGGTGGG and GAACTCAACCAGAGGGCCAA. The guides were cloned into plasmid pSpCas9n(BB)-2A-Puro (PX462) V2.0 (Feng Zhang Lab) obtained via Addgene, and equimolar amounts of plasmids were transfected using Lipofectamine 3000 (ThermoFisher). Cells harbouring at least one plasmid were enriched by selection with Puromycin at 1.5 µg ml^{-1} for 3-5 days and single cell sorted into 96-well plates containing growth medium, using a BD FACS Aria IIIU (BD Biosciences) with 85 µm nozzle. Single cells were grown out into clonal populations over a period of 10-14 days. Genetic loci harbouring insertion/deletion mutations (indels) were amplified by PCR using barcoded primers (AGTGACGGAGTGACTGACTG and GAGGTGAGGCCTACGTTGAT for *Anp32A*; TGTCTTGGACAATTGCAAATCAA and CCATGTGCTTTCTGCTACACT for *Anp32B*) (43).

282 A total 268 barcoded amplicons were then prepared for Next Generation sequencing using the
283 NEBNext Ultra II kit (NEB) and sequenced using 150-bp paired-end reads on an Illumina
284 MiSeq. Reads were mapped using BWA v0.7.5. Indels were detected when occurring above a
285 cut-off of 2.5% of reads using an R script (https://github.com/Flu1/CRISPR). NGS reads are
286 deposited in the European Nucleotide Archive (Project Number PRJEB31093). DNA sequences
287 were analysed in Geneious v6.

288 **Immunoblot analysis**

289 At least 250,000 cells were lysed in buffer containing 50 mM Tris-HCl pH 7.8 (Sigma Aldrich),
290 100 mM NaCl, 50 mM KCl and 0.5% Triton X-100 (Sigma Aldrich), supplemented with a
291 cOmplete™ EDTA free Protease inhibitor cocktail tablet (Roche) and prepared in Laemmli 2×
292 buffer (Sigma-Aldrich) after protein concentration had been established by spectrophotometry
293 (NanoDrop; ThermoFisher). Equal amounts of total protein were resolved by SDS–PAGE using
294 Mini PROTEAN TGX Precast Gels 4-20% (Bio-Rad). Immunoblotting by semi-dry transfer
295 (Bio-Rad Trans-Blot SD Semi-Dry Transfer Cell) onto nitrocellulose membranes (Amersham
296 Protran Premium 0.2 µm NC; GE Healthcare) was carried out using the following primary
297 antibodies: rabbit α-Vinculin (Abcam ab129002; 1/1,000), rabbit α-ANP32A (Abcam ab51013;
298 1/500), mouse α-ANP32B (Proteintech 66160-1-Ig 1/1,000) or rabbit α-ANP32B (Proteintech
299 10843-1-AP; 1/1,000), mouse α-IAV NP (Abcam ab128193; 1/1,000), mouse α-IBV NP (Abcam
300 ab20711; 1/1,000), mouse α-FLAG (F1804, Sigma-Aldrich; 1/500), and rabbit α-IAV PB2
301 (GTX125926, GeneTex; 1/4,000). The following secondary antibodies were used: sheep α-rabbit
302 HRP (AP510P, Merck; 1/10,000) and goat α-mouse HRP (STAR117P, AbD Serotec; 1/5,000).
303 Protein bands were visualized by chemiluminescence (ECL Prime Western Blotting Detection

Reagent; GE Healthcare) using a FUSION-FX imaging system (Vilber Lourmat). Western blots in Figures 1c-f, 2a-d, 5a, 6a-d, and 7c represent the accompanying minigenome assay; Western blots in Figures 1b are representative of at least 3 repeats.

Minigenome assay

In order to measure influenza virus polymerase activity, pCAGGS expression plasmids encoding PB1 (0.04 µg), PB2 (0.04 µg), PA (0.02 µg) and NP (0.08 µg) from each virus (H3N2 Victoria, H5N1 (PB2-627K) 50-92, pH1N1 England 195, or IBV Florida 06) were transfected into 200,000 eHAP1 or A549 cells using Lipofectamine 3000 (Thermo Fisher) at ratios of 2 µl P3000 reagent per µg plasmid DNA, and 3 µl Lipofectamine 3000 reagent per µg plasmid DNA. As reporter constructs, we transfected 0.04 µg PolI-luc, which encodes a minigenome containing a firefly reporter flanked by either influenza A or B promoter sequences, or PolI-BFP for Figure 2e. 0.04 µg pCAGGS-*Renilla* luciferase was transfected as a transfection and toxicity control. For exogenous expression, 0.1 ug pCAGGS plasmid encoding either the relevant FLAG-tagged *Anp32* gene, or Empty pCAGGS were co-expressed with the RNP components. The ratio of transfected plasmids was constant at all times with PB1 : PB2 : PA : NP : PolI reporter : *Renilla* : ANP32/Empty (if present) = 2:2:1:4:2:2:5 At least 20 hours post-transfection, cells were lysed in 100 µl Passive Lysis Buffer (Promega) and the Dual-Luciferase Reporter Assay kit (Promega) was used to measure bioluminescence on a FLUOstar Omega plate reader (BMG Labtech). In case of a PolI-BFP reporter please refer to fluorescence microscopy. All minigenome assays were repeated in triplicate at least twice.

Fluorescence microscopy

325 At least 200,000 cells were cultured on glass coverslips in 24-well plates and transfected or
326 infected as described. Cells transfected with plasmids encoding fluorescent proteins (BFP, GFP,
327 mCherry) were fixed in 4% paraformaldehyde and then visualised. Cells transfected with
328 plasmids encoding (FLAG-tagged) non-fluorescent proteins were fixed and permeabilized in
329 0.2% Triton X-100. Primary antibodies used were rabbit anti-FLAG F7425 (Sigma) or mouse
330 anti-IAV NP (Abcam 128193). Secondary antibodies were goat α-rabbit AlexaFluor-594
331 (ab150080, Invitrogen), or goat α-mouse AlexaFluor-568 (A11031, Invitrogen), respectively.
332 Coverslips were mounted on glass slides using Vectashield mounting medium (Vector
333 Laboratories H-1000-10). Cells were imaged with a Zeiss Cell Observer widefield microscope
334 with ZEN Blue software, using a Plan-Apochromat 100x, 1.40NA Oil objective (Zeiss), a
335 Hamamatsu ORCA-Flash 4.0 CMOS camera (frame 2048 x 2048 pixels), giving a pixel size of
336 65 nm, and a Colibri 7 light source (Zeiss). Channels acquired and filters for excitation and
337 emission were DAPI (ex 365/12 nm, em 447/60 nm), GFP (ex 470/40 nm, em 525/50 nm), and
338 TexasRed (ex 562/40 nm, em 624/40 nm). All images were analysed and prepared with Fiji
339 software (44). For images in Figures 2e) and S5b) the detection limit was adjusted individually
340 for each channel (taking care to remain well above control background level), while in Figure
341 3e), where we are comparing relative levels of NP expression, the lower detection limit in the
342 TexasRed channel was set equal to the DAPI channel.

343 **Influenza virus infection**

344 Cells were infected with virus diluted in serum free IMDM or DMEM at 37 °C (MOI as
345 indicated in the relevant figure legends) and replaced with serum-free cell culture medium
346 supplemented with 1 μg ml^{-1} TPCK trypsin (Worthington-Biochemical) after 1-2 hours. Cell

supernatants were harvested at indicated time points post-infection. Infectious titres were determined by plaque assay on MDCK cells. All virus infection assays were performed in triplicate at least twice; Figures 3a-d and S4 show one representative triplicate assay.

Safety/biosecurity

All work with infectious agents was conducted in biosafety level 2 facilities, approved by the Health and Safety Executive of the UK and in accordance with local rules, at Imperial College London, UK.

Viral RNA quantitation

Total RNA from 200,000 – 250,000 PR8-infected eHAP1 cells was extracted using the RNeasy mini kit (Qiagen), with 30 minutes on-column DNase I treatment (Qiagen). RNA concentrations were established by spectrophotometry (NanoDrop; Thermo Scientific), and equal amounts (500 ng) were subjected to cDNA synthesis using RevertAid reverse transcriptase (Thermo Scientific). PR8 segment 6 (NA) RNA species (vRNA, cRNA, and mRNA) were isolated using 5'-tagged primers (45) GGCCGTCATGGTGGCGAATGAAACCATAAAAAGTTGGAGGAAG, GCTAGCTTCAGCTAGGCATCAGTAGAAACAAGGAGTTTTTTGAAC, and CCAGATCGTTCGAGTCGTTTTTTTTTTTTTTTTGAACAGACTAC, respectively (tags underlined). Unique fragments of the NA gene were then amplified by real-time quantitative PCR using Fast SYBR Green Master Mix (Thermo Scientific), using the following primers: GGCCGTCATGGTGGCGAAT and CCTTCCCCTTTTCGATCTTG (vRNA – 148 bp), CTTTTTGTGGCGTGAATAGTG and GCTAGCTTCAGCTAGGCATC (cRNA – 108 bp), or CTTTTTGTGGCGTGAATAGTG and CCAGATCGTTCGAGTCGT (mRNA – 87 bp)

Quantitative PCR analysis was carried out on a Viia 7 Real-Time PCR System (Thermo Fisher). Gene expression was calculated by normalizing target gene expression to Ct values obtained in the mock-infected condition.

Bioinformatics

The alignment in Figure 4b was made in Clustal Omega, using primary sequences from Uniprot (P39687 (human ANP32A); Q92688 (human ANP32B); O35381 (mouse Anp32A); Q9EST5 (mouse Anp32B)).

Structural Modelling

To illustrate a chimeric construct with the LRR 5 from murine Anp32B in murine Anp32A we created a homology model of MusB obtained using iTASSER structural prediction software (based primarily on huANP32B-PDB 2RR6A and huANP32A-2JQDA; 2JEOA). The 3D structural model was visualised and created in UCSF Chimera; the LRR is shown in dark grey, the structurally unresolved LCAR in semi-transparent grey. Amino acid residues 128-153 are highlighted in blue and residue 130 in red stick format.

Acknowledgements

The authors wish to thank David Gaboriau for help with microscopy – the Facility for Imaging by Light Microscopy (FILM) at Imperial College London is part-supported by funding from the Wellcome Trust (grant 104931/Z/14/Z) and BBSRC (grant BB/L015129/1). We thank the St.

388 Mary's NHLI FACS core facility and Yanping Guo in particular for support and instrumentation,
389 and help with single cell sorting.

390 ES was supported by an Imperial College President's Scholarship; PJN, CMS, DHG, and WSB
391 were supported by Wellcome Trust grant 205100; BM was supported by a Wellcome Trust
392 Studentship; TPP was supported by Biotechnology and Biological Sciences Research Council
393 (BBSRC) grant BB/R013071/1; JSL and WSB were supported by BBSRC grant BB/K002465/1.

394 ES designed the research, performed experiments, and analysed data. PJN and BM performed
395 experiments and analysed data. CMS, TPP, and DHG analysed data. WSB and JSL designed the
396 research. ES, CMS, and WSB wrote the manuscript.

397

398

References

1. Iuliano AD, Roguski KM, Chang HH, Muscatello DJ, Palekar R, Tempia S, Cohen C, Gran JM, Schanzer D, Cowling BJ, Wu P, Kyncl J, Ang LW, Park M, Redlberger-Fritz M, Yu H, Espenhain L, Krishnan A, Emukule G, van Asten L, Pereira da Silva S, Aungkulanon S, Buchholz U, Widdowson MA, Bresee JS. 2018. Estimates of global seasonal influenza-associated respiratory mortality: a modelling study. Lancet 391:1285-1300.
2. Dawood FS, Iuliano AD, Reed C, Meltzer MI, Shay DK, Cheng PY, Bandaranayake D, Breiman RF, Brooks WA, Buchy P, Feikin DR, Fowler KB, Gordon A, Hien NT, Horby P, Huang QS, Katz MA, Krishnan A, Lal R, Montgomery JM, Molbak K, Pebody R, Presanis AM, Razuri H, Steens A, Tinoco YO, Wallinga J, Yu H, Vong S, Bresee J, Widdowson MA. 2012. Estimated global mortality associated with the first 12 months of 2009 pandemic influenza A H1N1 virus circulation: a modelling study. Lancet Infect Dis 12:687-95.
3. Hsu MT, Parvin JD, Gupta S, Krystal M, Palese P. 1987. Genomic RNAs of influenza viruses are held in a circular conformation in virions and in infected cells by a terminal panhandle. Proc Natl Acad Sci U S A 84:8140-4.
4. Moeller A, Kirchdoerfer RN, Potter CS, Carragher B, Wilson IA. 2012. Organization of the influenza virus replication machinery. Science 338:1631-4.
5. Arranz R, Coloma R, Chichon FJ, Conesa JJ, Carrascosa JL, Valpuesta JM, Ortin J, Martin-Benito J. 2012. The structure of native influenza virion ribonucleoproteins. Science 338:1634-7.
6. Pflug A, Guilligay D, Reich S, Cusack S. 2014. Structure of influenza A polymerase bound to the viral RNA promoter. Nature 516:355-60.
7. Te Velthuis AJ, Fodor E. 2016. Influenza virus RNA polymerase: insights into the mechanisms of viral RNA synthesis. Nat Rev Microbiol 14:479-93.
8. Pflug A, Lukarska M, Resa-Infante P, Reich S, Cusack S. 2017. Structural insights into RNA synthesis by the influenza virus transcription-replication machine. Virus Res doi:10.1016/j.virusres.2017.01.013.
9. Reilly PT, Yu Y, Hamiche A, Wang L. 2014. Cracking the ANP32 whips: important functions, unequal requirement, and hints at disease implications. Bioessays 36:1062-71.
10. Seo SB, McNamara P, Heo S, Turner A, Lane WS, Chakravarti D. 2001. Regulation of histone acetylation and transcription by INHAT, a human cellular complex containing the set oncoprotein. Cell 104:119-30.
11. Fan Z, Zhang H, Zhang Q. 2006. Tumor suppressor pp32 represses cell growth through inhibition of transcription by blocking acetylation and phosphorylation of histone H3 and initiating its proapoptotic activity. Cell Death Differ 13:1485-94.
12. Fan Z, Beresford PJ, Oh DY, Zhang D, Lieberman J. 2003. Tumor suppressor NM23-H1 is a granzyme A-activated DNase during CTL-mediated apoptosis, and the nucleosome assembly protein SET is its inhibitor. Cell 112:659-72.
13. Schafer ZT, Parrish AB, Wright KM, Margolis SS, Marks JR, Deshmukh M, Kornbluth S. 2006. Enhanced sensitivity to cytochrome c-induced apoptosis mediated by PHAPI in breast cancer cells. Cancer Res 66:2210-8.
14. Munemasa Y, Suzuki T, Aizawa K, Miyamoto S, Imai Y, Matsumura T, Horikoshi M, Nagai R. 2008. Promoter region-specific histone incorporation by the novel histone chaperone ANP32B and DNA-binding factor KLF5. Mol Cell Biol 28:1171-81.
15. Cvetanovic M, Rooney RJ, Garcia JJ, Toporovskaya N, Zoghbi HY, Opal P. 2007. The role of LANP and ataxin 1 in E4F-mediated transcriptional repression. EMBO Rep 8:671-7.

16. Brennan CM, Gallouzi IE, Steitz JA. 2000. Protein ligands to HuR modulate its interaction with target mRNAs in vivo. J Cell Biol 151:1-14.
17. Sugiyama K, Kawaguchi A, Okuwaki M, Nagata K. 2015. pp32 and APRIL are host cell-derived regulators of influenza virus RNA synthesis from cRNA. Elife 4.
18. Long JS, Giotis ES, Moncorge O, Frise R, Mistry B, James J, Morisson M, Iqbal M, Vignal A, Skinner MA, Barclay WS. 2016. Species difference in ANP32A underlies influenza A virus polymerase host restriction. Nature 529:101-4.
19. Baker SF, Ledwith MP, Mehle A. 2018. Differential Splicing of ANP32A in Birds Alters Its Ability to Stimulate RNA Synthesis by Restricted Influenza Polymerase. Cell Rep 24:2581-2588.e4.
20. Domingues P, Hale BG. 2017. Functional Insights into ANP32A-Dependent Influenza A Virus Polymerase Host Restriction. Cell Rep 20:2538-2546.
21. Watanabe T, Kawakami E, Shoemaker JE, Lopes TJ, Matsuoka Y, Tomita Y, Kozuka-Hata H, Gorai T, Kuwahara T, Takeda E, Nagata A, Takano R, Kiso M, Yamashita M, Sakai-Tagawa Y, Katsura H, Nonaka N, Fujii H, Fujii K, Sugita Y, Noda T, Goto H, Fukuyama S, Watanabe S, Neumann G, Oyama M, Kitano H, Kawaoka Y. 2014. Influenza virus-host interactome screen as a platform for antiviral drug development. Cell Host Microbe 16:795-805.
22. Bradel-Tretheway BG, Mattiacio JL, Krasnoselsky A, Stevenson C, Purdy D, Dewhurst S, Katze MG. 2011. Comprehensive proteomic analysis of influenza virus polymerase complex reveals a novel association with mitochondrial proteins and RNA polymerase accessory factors. J Virol 85:8569-81.
23. Long JS, Mistry B, Haslam SM, Barclay WS. 2019. Host and viral determinants of influenza A virus species specificity. Nature Reviews Microbiology 17:67-81.
24. Essletzbichler P, Konopka T, Santoro F, Chen D, Gapp BV, Kralovics R, Brummelkamp TR, Nijman SM, Burckstummer T. 2014. Megabase-scale deletion using CRISPR/Cas9 to generate a fully haploid human cell line. Genome Res 24:2059-65.
25. Carette JE, Raaben M, Wong AC, Herbert AS, Obernosterer G, Mulherkar N, Kuehne AI, Kranzusch PJ, Griffin AM, Ruthel G, Dal Cin P, Dye JM, Whelan SP, Chandran K, Brummelkamp TR. 2011. Ebola virus entry requires the cholesterol transporter Niemann-Pick C1. Nature 477:340-3.
26. Ran FA, Hsu PD, Lin CY, Gootenberg JS, Konermann S, Trevino AE, Scott DA, Inoue A, Matoba S, Zhang Y, Zhang F. 2013. Double nicking by RNA-guided CRISPR Cas9 for enhanced genome editing specificity. Cell 154:1380-9.
27. Ran FA, Hsu PD, Wright J, Agarwala V, Scott DA, Zhang F. 2013. Genome engineering using the CRISPR-Cas9 system. Nat Protoc 8:2281-2308.
28. Doench JG, Fusi N, Sullender M, Hegde M, Vaimberg EW, Donovan KF, Smith I, Tothova Z, Wilen C, Orchard R, Virgin HW, Listgarten J, Root DE. 2016. Optimized sgRNA design to maximize activity and minimize off-target effects of CRISPR-Cas9. Nat Biotechnol 34:184-91.
29. Jorba N, Coloma R, Ortin J. 2009. Genetic trans-complementation establishes a new model for influenza virus RNA transcription and replication. PLoS Pathog 5:e1000462.
30. York A, Hengrung N, Vreede FT, Huiskonen JT, Fodor E. 2013. Isolation and characterization of the positive-sense replicative intermediate of a negative-strand RNA virus. Proc Natl Acad Sci U S A 110:E4238-45.
31. Zhang H, Zhang Z, Wang Y, Wang M, Wang X, Zhang X, Ji S, Du C, Chen H, Wang X. 2019. Fundamental contribution and host range determination of ANP32A and ANP32B in influenza A virus polymerase activity. Journal of Virology doi:10.1128/jvi.00174-19:JVI.00174-19.
32. Long JS, Idoko-Akoh A, Mistry B, Goldhill D, Staller E, Schreyer J, Ross C, Goodbourn S, Shelton H, Skinner MA, Sang H, McGrew MJ, Barclay W. 2019. Species specific differences in use of ANP32 proteins by influenza A virus. eLife 8:e45066.

33. Karlas A, Machuy N, Shin Y, Pleissner KP, Artarini A, Heuer D, Becker D, Khalil H, Ogilvie LA, Hess S, Maurer AP, Muller E, Wolff T, Rudel T, Meyer TF. 2010. Genome-wide RNAi screen identifies human host factors crucial for influenza virus replication. Nature 463:818-22.
34. Han J, Perez JT, Chen C, Li Y, Benitez A, Kandasamy M, Lee Y, Andrade J, tenOever B, Manicassamy B. 2018. Genome-wide CRISPR/Cas9 Screen Identifies Host Factors Essential for Influenza Virus Replication. Cell Rep 23:596-607.
36. Goldhill DH, Te Velthuis AJW, Fletcher RA, Langat P, Zambon M, Lackenby A, Barclay WS. 2018. The mechanism of resistance to favipiravir in influenza. Proc Natl Acad Sci U S A 115:11613-11618.
37. Bloom JD, Gong LI, Baltimore D. 2010. Permissive secondary mutations enable the evolution of influenza oseltamivir resistance. Science 328:1272-5.
38. Bright RA, Shay DK, Shu B, Cox NJ, Klimov AI. 2006. Adamantane resistance among influenza A viruses isolated early during the 2005-2006 influenza season in the United States. Jama 295:891-4.
39. Takashita E, Morita H, Ogawa R, Nakamura K, Fujisaki S, Shirakura M, Kuwahara T, Kishida N, Watanabe S, Odagiri T. 2018. Susceptibility of Influenza Viruses to the Novel Cap-Dependent Endonuclease Inhibitor Baloxavir Marboxil. Front Microbiol 9:3026.
40. Long JS, Howard WA, Nunez A, Moncorge O, Lycett S, Banks J, Barclay WS. 2013. The effect of the PB2 mutation 627K on highly pathogenic H5N1 avian influenza virus is dependent on the virus lineage. J Virol 87:9983-96.
41. Moncorge O, Long JS, Cauldwell AV, Zhou H, Lycett SJ, Barclay WS. 2013. Investigation of influenza virus polymerase activity in pig cells. J Virol 87:384-94.
42. Jackson D, Cadman A, Zurcher T, Barclay WS. 2002. A reverse genetics approach for recovery of recombinant influenza B viruses entirely from cDNA. J Virol 76:11744-7.
43. Bystrykh LV. 2012. Generalized DNA barcode design based on Hamming codes. PLoS One 7:e36852.
44. Schindelin J, Arganda-Carreras I, Frise E, Kaynig V, Longair M, Pietzsch T, Preibisch S, Rueden C, Saalfeld S, Schmid B, Tinevez JY, White DJ, Hartenstein V, Eliceiri K, Tomancak P, Cardona A. 2012. Fiji: an open-source platform for biological-image analysis. Nat Methods 9:676-82.
45. Kawakami E, Watanabe T, Fujii K, Goto H, Watanabe S, Noda T, Kawaoka Y. 2011. Strand-specific real-time RT-PCR for distinguishing influenza vRNA, cRNA, and mRNA. J Virol Methods 173:1-6.
46. Knyaz C, Stecher G, Li M, Kumar S, Tamura K. 2018. MEGA X: Molecular Evolutionary Genetics Analysis across Computing Platforms. Molecular Biology and Evolution 35:1547-1549.

526 **Figure legends**

527 **Figure 1. Human cells lacking ANP32A and ANP32B do not support influenza virus**
528 **polymerase activity**

529 a) Schematic showing location of CRISPR guide RNA target sequences in the gene structure of
530 human ANP32A or B b) Western blotting analysis showing ANP32A (upper panels) or B (lower
531 panels) expression in eHAP1 control, single (AKO 18 and BKO 20) and double (dKO 26)
532 knockout cells c-f) Minigenome assays in eHAP1 control, AKO, BKO, or dKO cells. Cells were
533 transfected with plasmids to reconstitute polymerase from H3N2 Victoria (c), H5N1 50-92 (PB2
534 627K) (d), pH1N1 England 195 (e), or IBV Florida 06 (f) virus, along with IAV or IBV firefly
535 minigenome reporter, and *Renilla* expression control. Data shown are firefly activity normalised
536 to *Renilla*, plotted as mean (SD) obtained by one-way ANOVA from one representative repeat
537 (N > 3). Accompanying Western blots show expression of respective vRNP components in each
538 cell type (representative of one minigenome assay). ns = not significant; *p<0.05; **p<0.01;
539 ***p<0.001; ****p<0.0001

540 **Figure 2. Exogenous ANP32 expression recovers polymerase activity in dKO cells.**

541 a-d) Minigenome assays in eHAP1 dKO cells with co-expressed Empty vector (Empty), FLAG-
542 tagged ANP32A, ANP32B, or ANP32A and ANP32B expression plasmids. Accompanying
543 Western blots show expression of FLAG-tagged ANP32 constructs alongside respective vRNP
544 components (representative of one minigenome assay). Data shown are firefly activity
545 normalised to *Renilla* plotted as mean (SD) obtained by one-way ANOVA from one
546 representative repeat (N > 3). ns = not significant; **p<0.01; **** p<0.0001 e) Expression from
547 IAV minigenome encoding NLS-tagged BFP in eHAP1 dKO cells exogenously reconstituted

548 with mCherry-tagged ANP32A or B. Cells were transfected with expression plasmids encoding
549 50-92 PB1, PB2 627K, PA-GFP, as well as NP, and either mCherry-tagged ANP32A or B and a
550 blue fluorescent protein (BFP-NLS) minigenome reporter.

551 **Figure 3. IAV replication is abrogated in dKO cells.**

552 a-c) Control (black), AKO (red), BKO (blue), and dKO (purple) cells were infected with H3N2
553 Victoria 6:2 reassortant virus with PR8 HA and NA genes, H5N1 A/Tky/50-92 (PB2-627K) 5:3
554 reassortant with PR8 HA, NA, and M genes, or pH1N1 England 195, respectively (MOI 0.005)
555 and incubated at 37°C in the presence of 1μg/ml trypsin to allow multicycle replication.
556 Supernatants were harvested at the indicated days post infection (dpi) and PFU ml^{-1} established
557 by plaque assay on MDCK cells. d) dKO cells were transfected with equimolar amount of
558 ANP32A and ANP32B expression plasmids 6 h prior to infection with H1N1 PR8 virus (MOI
559 0.005). Cells were incubated at 37°C in the presence of 1μg/ml trypsin and supernatants
560 collected at indicated time points. Data shown are mean PFU ml^{-1} measured by plaque assay on
561 MDCK cells. LOD (dotted line) denotes the limit of detection based on the dilution factor in
562 plaque assays. All infection experiments were repeated at least twice. Graphs shown are one
563 representative triplicate assay. Statistical significance was calculated per time point by Student t-
564 test. ns = not significant; *p<0.05; **p<0.01; ***p<0.001; ****p<0.0001

565

566 **Figure 4. Synthesis of vRNA from cRNA template is abrogated in cells lacking ANP32A**
567 **and B.**

568 a) Immunofluorescence analysis for NP expression in control cells, dKO or mock-infected cells.
569 Cells were infected with H1N1 PR8 virus (MOI 0.2) for 5 hours in growth medium, then fixed

570 and incubated with primary α-IAV NP antibody followed by AlexaFluor-568 secondary antibody
571 and imaged on a Zeiss Cell Observer widefield microscope. The lower detection limit in the
572 TexasRed channel was set to the DAPI channel. b) b) qRT-PCR analysis demonstrating
573 accumulation of PR8 virus segment 6 vRNA, cRNA, and mRNA in the absence or presence of
574 100 µg ml^{-1} cycloheximide (CHX). eHAP1 control or dKO cells were transfected with H5N1
575 Tky/50-92 polymerase components PB1-D446Y (catalytically inactive), PB2-627K, and PA in a
576 1:1:1 ratio 20 hours prior to infection with PR8 virus at MOI = 10. RNA was extracted 5 hours
577 post-infection. Data show mean (SD) of 40-Ct values normalised to mean mock-infected levels,
578 analysed per cell type by one-way ANOVA. Experimental data representative of 3 repeats. ns =
579 not significant; *** $p<0.001$; **** $p<0.0001$

580

581 Figure 5. **Influenza A virus polymerase activity is supported by murine Anp32B but not A.**

582 a)Minigenome reporter assay in dKO cells with co-transfected FLAG-tagged Anp32A from pig
583 (SusA), mouse (MusA), duck (AnasA), or chicken (GallusA) with H3N2 Victoria RNP
584 components, pPolI-firefly minigenome reporter, and *Renilla* transcription control. Data show
585 mean (SD) of firefly activity normalised to *Renilla* analyzed by one-way ANOVA from one
586 representative repeat (N = 2 triplicate experiments). ns = not significant; ****$p<0.0001$.
587 Accompanying Western blot shows expression of vRNP component PB2 and co-expressed
588 FLAG-tagged ANP32 constructs b) Minigenome assay showing activity of Vic/75 polymerase in
589 eHPA1 dKO cells co-expressing mouse Anp32A, Anp32B, or $Anp32A^{128-153}$ Data were analysed
590 as above. Accompanying Western blot shows expression of vRNP component PB2 and co-
591 expressed FLAG-tagged ANP32 constructs c) Immunofluorescence analysis showing expression
592 of FLAG-tagged MusA, MusB, and $MusA^{128-153}$ detected with anti-FLAG antibody and

AlexaFluor-594 anti-rabbit conjugate and counterstained with DAPI. d) Cartoon showing chimeric mouse ANP32 protein with 26 amino acids from mouse Anp32A LRR 5 replaced by the equivalent sequence from mouse Anp32B e) structural model of mouse Anp32B highlighting the swapped domain in blue (LRR in dark grey, LCAR in semi-transparent grey, and the domain swap in blue with amino acid 130 represented as a red stick) f) Alignment comparing LRR 5 amino acid sequence of mouse Anp32A to its -B homologue, human ANP32A, and human ANP32B g) Minigenome assay for activity of H3N2 Victoria polymerase in eHAP1 dKO cells co-expressing wildtype human or mouse ANP32A, or position 130 point mutants. Data show mean (SD) of firefly activity normalised to *Renilla* analyzed by one-way ANOVA from one representative repeat (N = 3 triplicate experiments). ** $p<0.01$; **** $p<0.0001$. Accompanying Western blot shows expression of vRNP component PB2 and co-expressed FLAG-tagged ANP32 constructs

Figure 6. Murine Anp32A can support IBV but not IAV polymerase activity

Minigenome assays in eHAP1 dKO cells showing activity of polymerases from H5N1 Tky/50-92 (PB2-627K) (a), pH1N1 Eng/195 (b), and B/Florida/06 co-transfected with FLAG-tagged mouse Anp32A, Anp32B, or Anp32A$^{128\text{-}153}$. Data show mean (SD) of firefly activity normalised to *Renilla* analyzed by one-way ANOVA from one representative repeat (N = 2 triplicate experiments). ns = not significant; * $p<0.05$; **** $p<0.0001$. Accompanying Western blot shows expression of vRNP component PB2 and co-expressed FLAG-tagged ANP32 constructs

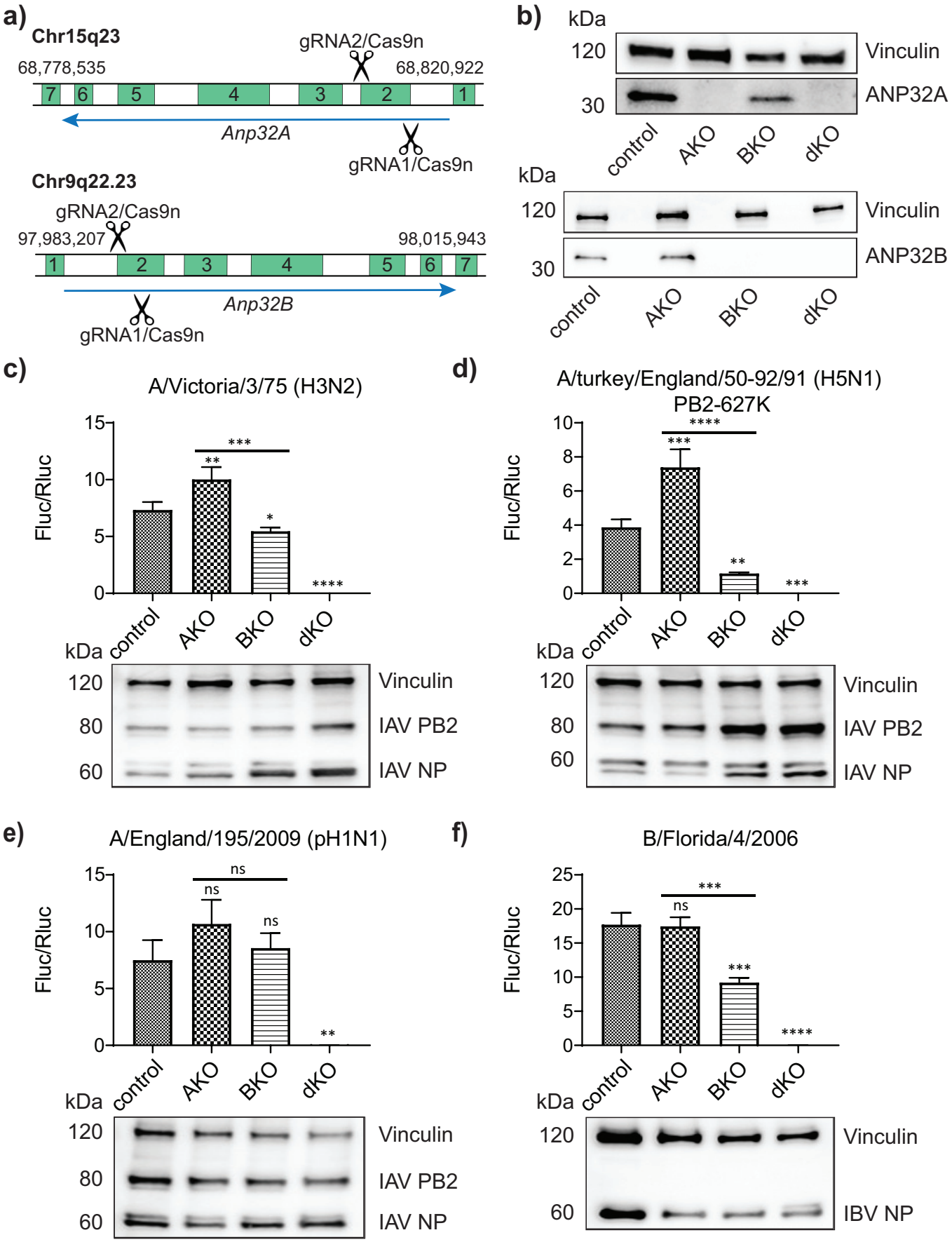

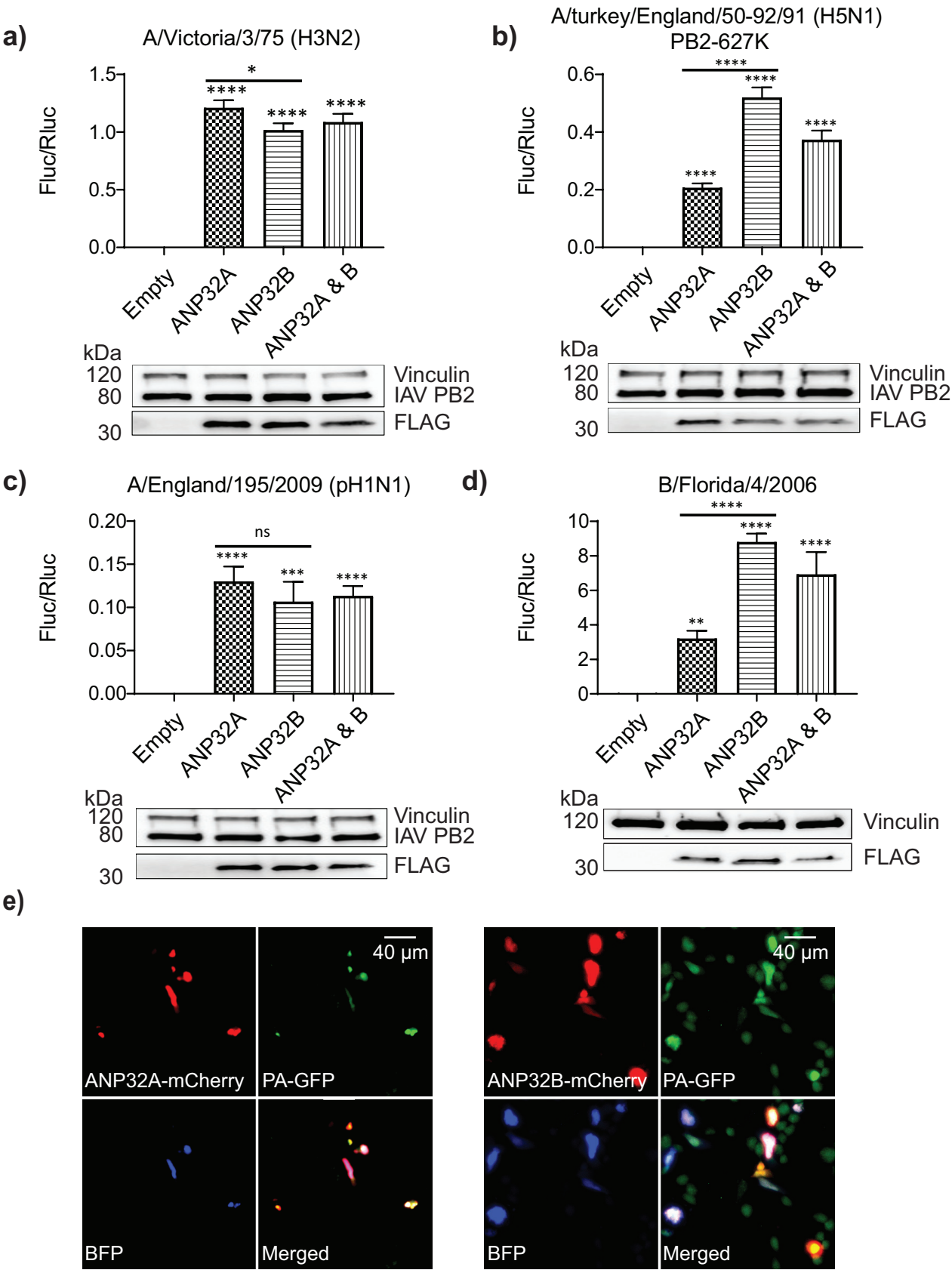

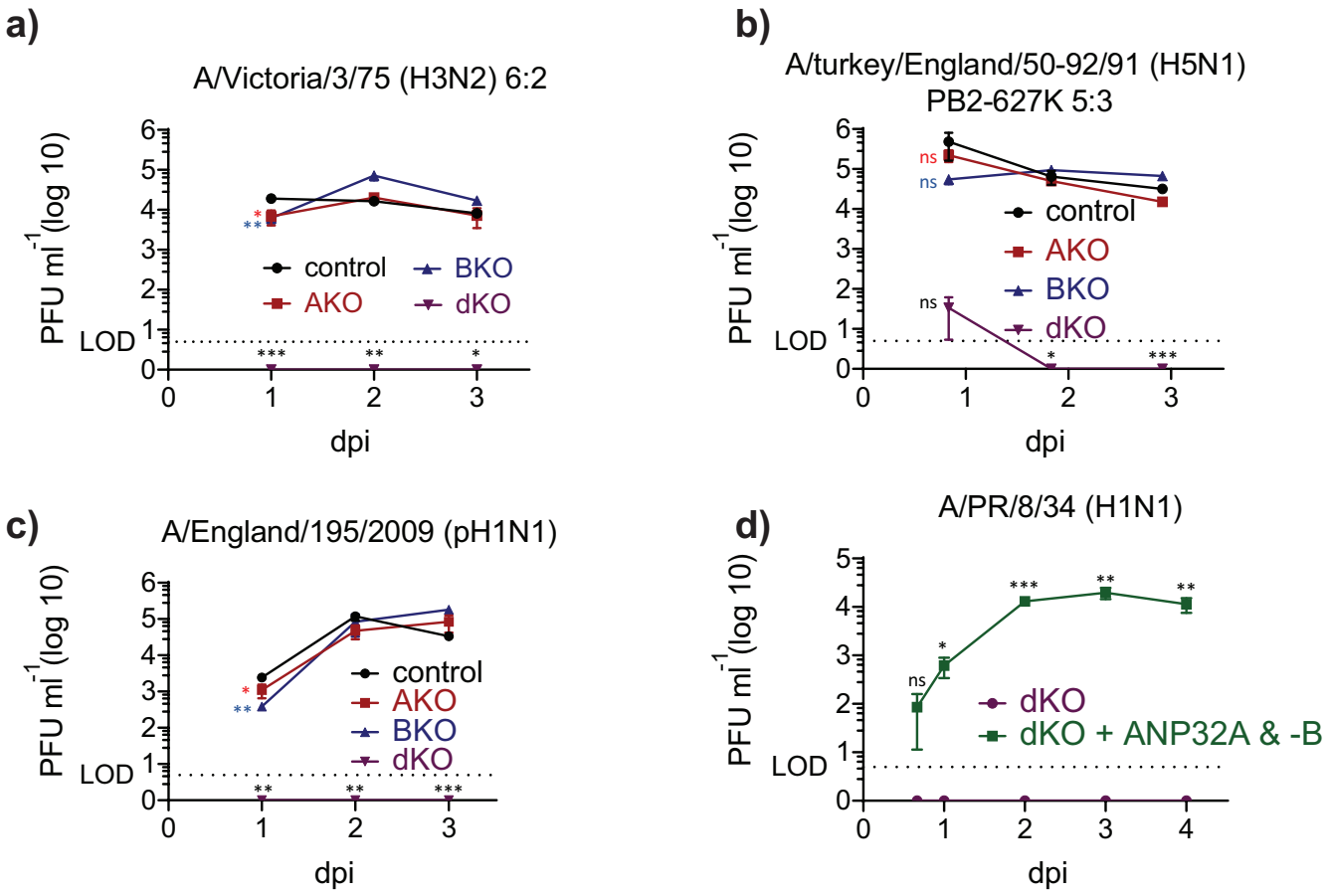

a)

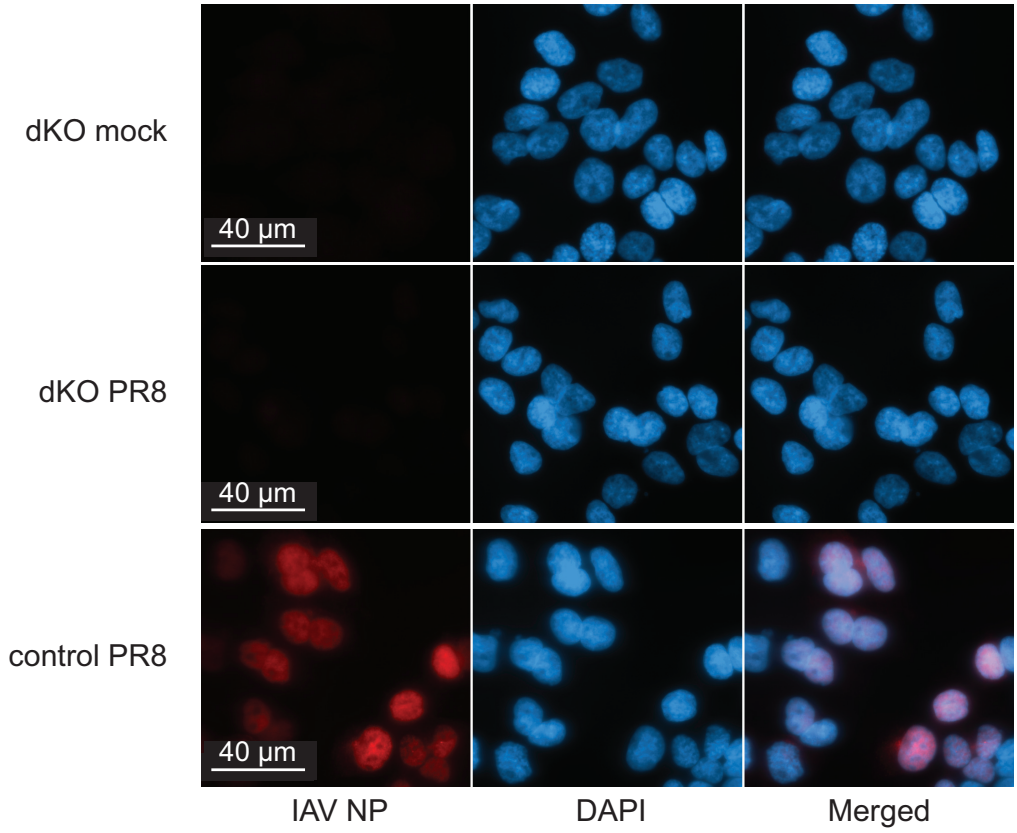

b)

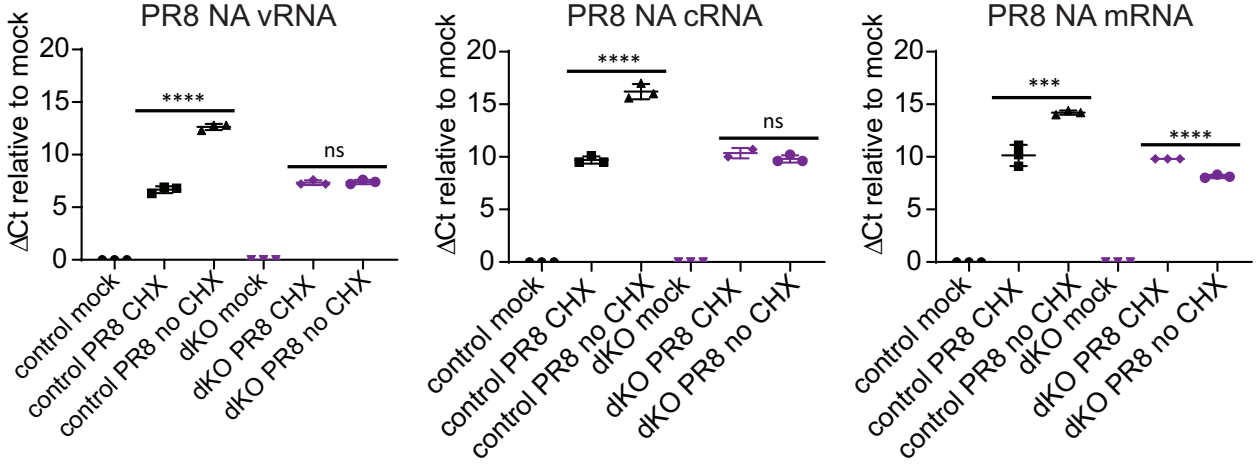

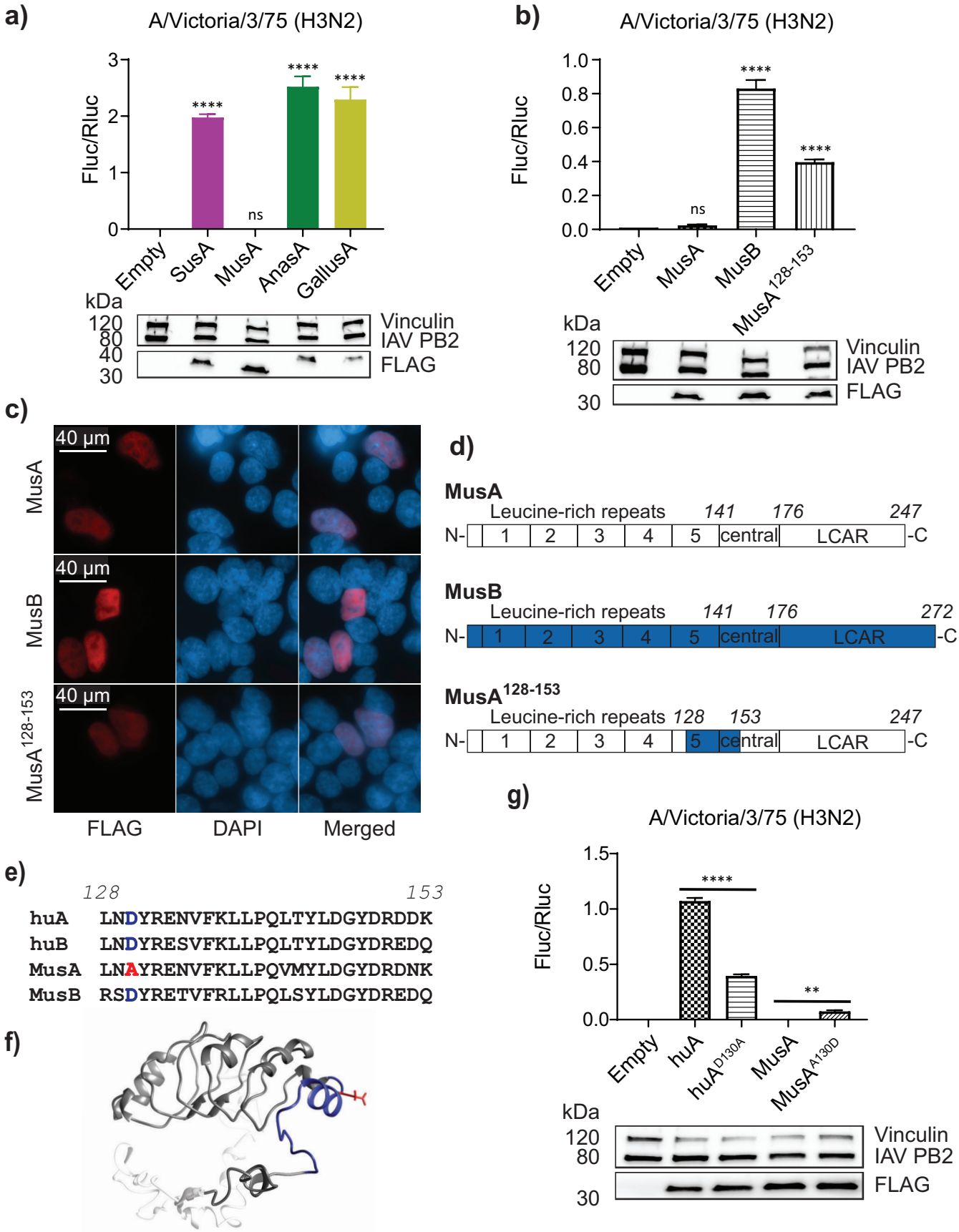

a)

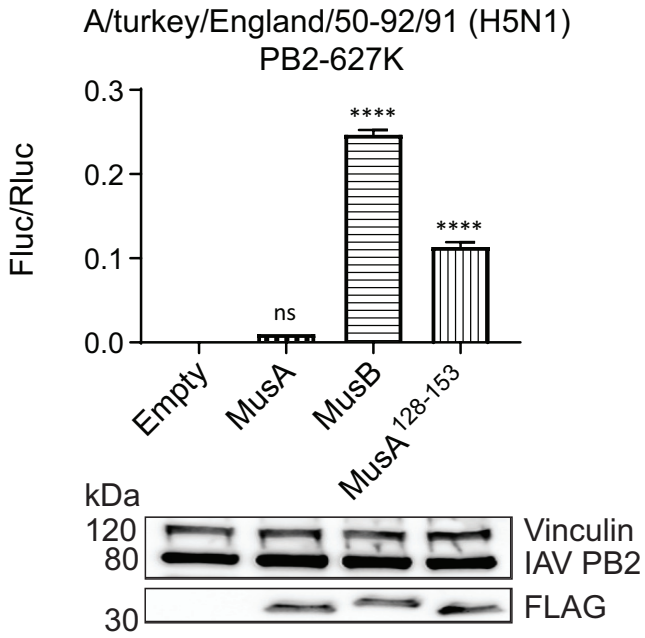

b)

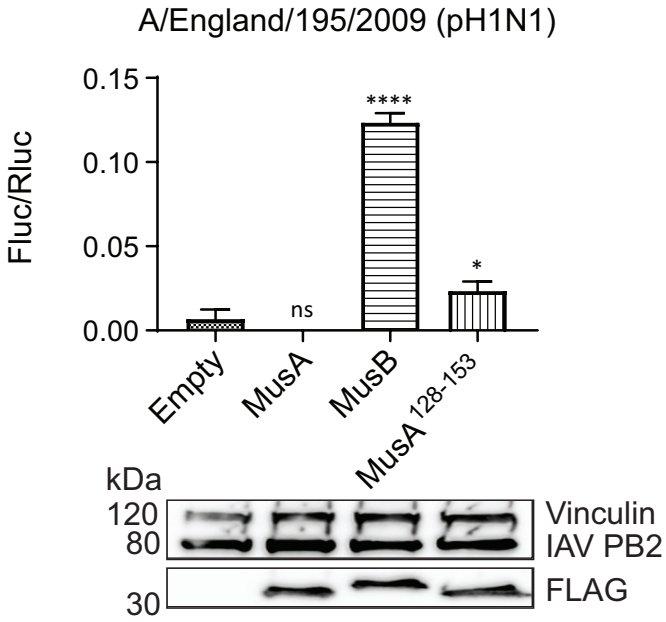

c)